



## Study the optical properties of $\text{GdVO}_4:5\%\text{Eu}^{3+}$ towards application for WLEDs in agriculture

Ngo Quoc Luan<sup>1</sup>, Ngo Khắc Khong Minh<sup>2\*</sup>, Nguyen Thi Thu Huong<sup>1</sup>, Phan Thanh Phuong<sup>1</sup>,  
 Le Van Ril<sup>3</sup>, Le Van Phuong<sup>4</sup>, Nguyen Van Minh Em<sup>5</sup>, Nguyen Vu<sup>6</sup>

<sup>1</sup> School of Education, Can Tho University, Can Tho, Vietnam

<sup>2</sup> Scientific Management-International Relations Department, Can Tho University of Technology, Can Tho, Vietnam

<sup>3</sup> Medical faculty, Nam Can Tho University, Can Tho, Vietnam

<sup>4</sup> FPT High School, Can Tho, Vietnam

<sup>5</sup> Le Hoai Don High School, Ben Tre, Vietnam

<sup>6</sup> Institute of Materials Science, Vietnam Academy of Science and Technology, Vietnam

\* Email: [nkkminh@ctu.edu.vn](mailto:nkkminh@ctu.edu.vn)

### ARTICLE INFO

Received: 17/04/2024

Accepted: 16/05/2024

Published: 30/03/2025

Keywords:

$\text{GdVO}_4:\text{Eu}^{3+}$ ; luminescence;  
 combustion synthesis;  
 optical nanomaterials;  
 WLEDs in agriculture

### ABSTRACT

In this study, we synthesized  $\text{GdVO}_4:5\%\text{Eu}^{3+}$  using a straightforward combustion method. The structures, chemical composition, and optical properties of this material were analyzed through X-ray diffraction (XRD), energy-dispersive X-ray (EDX), and photoluminescence (PL) spectra. The emission spectra, observed under 470 nm excitation, correspond to the  ${}^5\text{D}_0 - {}^7\text{F}_J$  ( $J = 0-4$ ) transition of the  $\text{Eu}^{3+}$  ion, resulting in red emission within the 590-700 nm region, aligning with the light absorption spectrum of plants. WLED devices were fabricated using  $\text{GdVO}_4:5\%\text{Eu}^{3+}$  and  $\text{YAG}:\text{Ce}^{3+}$  powders towards agricultural purposes. The color coordinates of the resulting WLED were (0.319, 0.323), close to the standard white emission coordinate (0.333, 0.333).

### Introduction

For decades, luminescent nanomaterials containing rare earth ions have been a focal point for scientists due to their numerous practical applications in artificial optical devices [1,2]. Recently, these nanomaterials have found new use in specialized light bulbs for agricultural purposes, aimed at enhancing crop productivity [3]. Despite the rise of energy-saving and environmentally friendly lighting solutions like LED lights, conventional lighting devices are inadequate for plant growth. This is because their visible light absorption spectrum falls outside the optimal range for plant photosynthesis, which is primarily between 400 - 700 nm, with peaks in the red (600 - 700 nm) and blue (400 - 500 nm) regions [4,5]. Consequently, the

challenge lies in developing lamps tailored specifically for plants, emitting light within the spectra conducive to plant absorption.

The  $\text{GdVO}_4:\text{Eu}^{3+}$  material has gained considerable scientific interest, particularly following Nguyen Vu's successful synthesis of  $\text{GdVO}_4:5\%\text{Eu}^{3+}$  via the hydrothermal method in 2015, which examined its optical properties [6]. Their study demonstrated that upon excitation at 310 nm, the material emits red light within the 593-699 nm range, corresponding to the  ${}^5\text{D}_0 - {}^7\text{F}_J$  ( $J=1-4$ ) transitions of  $\text{Eu}^{3+}$  ions, highlighting its potential for agricultural lighting applications. Furthermore, in 2020, N.K.K. Minh synthesized  $\text{Gd}_3\text{PO}_7:1\%\text{Eu}$  using the combustion method and identified 900°C as the optimal temperature for material synthesis [11]. Based on these insights, our

<https://doi.org/10.62239/jca.2025.002>

current research employs a calcination temperature of 900°C and  $\text{Eu}^{3+}$  ions doping concentration of 5 mol% to synthesize the material. We are investigating its structural and optical properties, and have conducted initial tests by coating 470 nm LED chips with  $\text{GdVO}_4:5\%\text{Eu}^{3+}$  nano powder for potential use in LED lights tailored for agricultural applications.

## Experimental

The nanomaterial  $\text{GdVO}_4:5\%\text{Eu}^{3+}$  was produced using gadolinium (III) oxide ( $\text{Gd}_2\text{O}_3$  99.9%), europium(III) oxide ( $\text{Eu}_2\text{O}_3$  99.99%),  $\text{NH}_4\text{VO}_3$ , and urea. Initially,  $\text{Gd}_2\text{O}_3$  and  $\text{Eu}_2\text{O}_3$  were dissolved in concentrated  $\text{HNO}_3$  to form rare earth nitrate solutions. The mixture of  $\text{Gd}(\text{NO}_3)_3$  and  $\text{Eu}(\text{NO}_3)_3$  (with a molar ratio of  $\text{Gd}^{3+}$  ion to  $\text{Eu}^{3+}$  ion of 95:5) was evaporated three times, followed by the addition of distilled water. Urea was then added as a fuel and stirred until a colorless solution (solution A) was obtained.  $\text{NH}_4\text{VO}_3$  was dissolved in distilled water at 70°C to produce a clear yellow solution (solution B). Solution B was slowly added to solution A with stirring for 1 hour. The resulting mixture was evaporated to yield a yellow gel (precursor), which was subsequently heated to 900°C at a rate of 10°C/min.

X-ray diffraction analysis was conducted using a D8 ADVANCE Bruker machine at the Institute of Chemistry, Vietnam Academy of Science and Technology. Energy dispersive X-ray spectroscopy (EDX) was performed using a FESEM HITACHI S-4800 machine at the Institute of Materials Science, Vietnam Academy of Science and Technology. Fluorescence excitation spectrum and fluorescence spectrum measurements were carried out using a Fluorolog-3 device at the Institute of Chemistry, Vietnam Academy of Science and Technology. The electro-luminescent spectra of the LED devices were recorded on LED Testing Systems (Gamma Scientific), Hanoi University of Science and Technology.

## Results and discussion

Fig. 1 depicts the X-ray diffraction (XRD) pattern of  $\text{GdVO}_4$  doped with 5 mol%  $\text{Eu}^{3+}$ . The pattern confirms that the synthesized material is  $\text{GdVO}_4$  single-phase, no peaks of other phases could be observed. All diffraction peaks align with the JCPDS 17-1260 standard card for  $\text{GdVO}_4$ , both in position and intensity ratio. Some characteristic diffraction lines are at  $2\theta = 24.67^\circ$ ,  $31.09^\circ$ ,  $33.23^\circ$ ,  $35.15^\circ$ ,  $37.72^\circ$ ,  $40.07^\circ$  and  $49.17^\circ$

corresponding to (200), (211), (112), (220), (202), (301) and (312) planes of  $\text{GdVO}_4$ , respectively [7,8]. Additionally, the pattern indicates that the doping of a small amount of Eu into the  $\text{GdVO}_4$  structure does not effect on the material structure. The average particle size is 34 nm, calculated using the Debye-Scherrer formula with equation  $D=0.89\lambda/\beta\cos\theta$ . where  $D$  is the average crystal size,  $\lambda$  is the wavelength of the Cu  $\text{K}\alpha$  radiation,  $\theta$  is the Bragg angle and  $\beta$  represents the full-width at half maximum (FWHM) in radians of the peak at  $2\theta = 24.67^\circ$ .

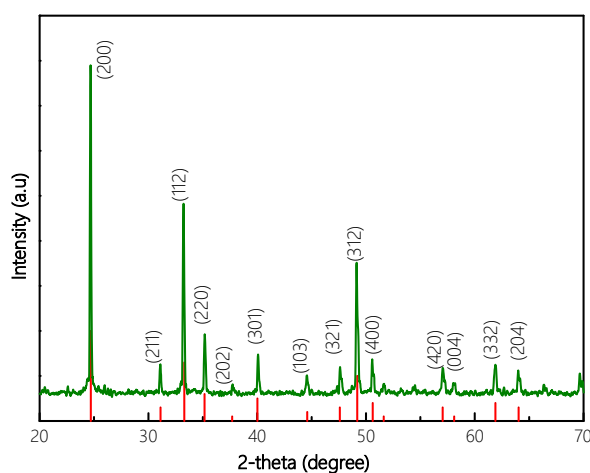


Fig. 1. XRD pattern of  $\text{GdVO}_4$  doped with 5 mol%  $\text{Eu}^{3+}$

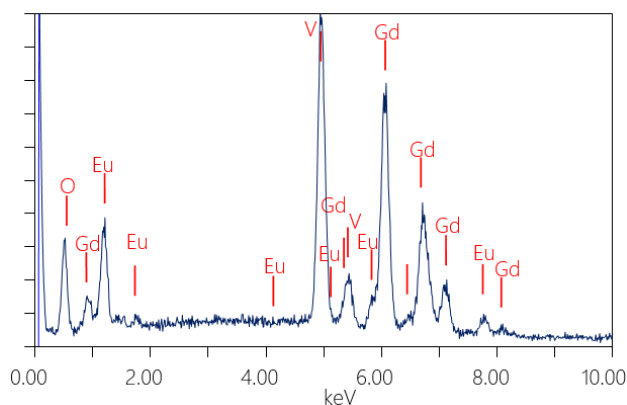


Fig. 2. EDX spectrum of the  $\text{GdVO}_4:5\%\text{Eu}^{3+}$

The EDX (energy dispersive X-ray) spectrum shown in Fig. 2 for the  $\text{GdVO}_4:5\%\text{Eu}^{3+}$  material confirms the presence of gadolinium (Gd), vanadium (V), oxygen (O), and europium (Eu) in the sample. The peak intensity corresponds to the concentration of each element. Notably, no impurities are detected, indicating the material's purity. The atomic mole percentages of Gd, Eu, V, and O are 16.29%, 0.96%, 16.42%, and 66.32%, respectively, closely matching the calculated ratio for  $\text{GdVO}_4$ .

Fig. 3 displays the fluorescence excitation spectrum of both  $\text{GdVO}_4:5\%\text{Eu}^{3+}$  and pure  $\text{GdVO}_4$  materials. Notably, the spectrum exhibits a broad band in the shorter wavelength range (250-350 nm), known as the charge transfer region (CTB). The initial broad band around 315 nm is associated with the absorption of the vanadate group, wherein electrons undergo a transition from the 2p orbital of oxygen to the 3d orbital of vanadium. This feature is evident in both the  $\text{GdVO}_4:\text{Eu}^{3+}$  and  $\text{GdVO}_4$  curves. Furthermore, an additional signal was observed at approximately 280 nm in the excitation spectrum of  $\text{GdVO}_4:\text{Eu}^{3+}$ , identified as the Eu-O charge transfer region [9,10]. Additionally, narrow lines appear in the 350 to 500 nm range, indicative of f-f transitions of  $\text{Eu}^{3+}$  ions. Specifically, these lines correspond to excitation wavelengths of 364, 382, 395, 417, and 470 nm, corresponding to the  ${}^7\text{F}_0 - {}^5\text{D}_4$ ,  ${}^7\text{F}_0 - {}^5\text{G}_2$ ,  ${}^7\text{F}_0 - {}^5\text{L}_6$ ,  ${}^7\text{F}_0 - {}^5\text{D}_3$ , and  ${}^7\text{F}_0 - {}^5\text{D}_2$  transitions, respectively [11-13].

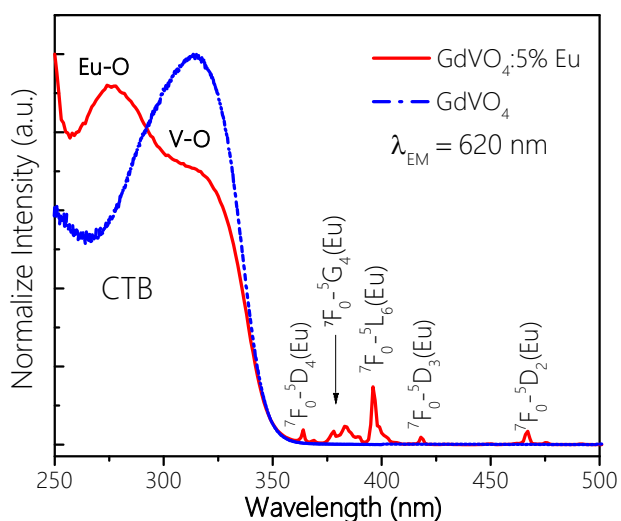


Fig.3. Photoluminescence excitation spectra (PLE) of  $\text{GdVO}_4:5\%\text{Eu}^{3+}$

The fluorescence spectrum of the  $\text{GdVO}_4:5\%\text{Eu}^{3+}$  material under an excitation wavelength of 470 nm, as depicted in Fig. 4, reveals narrow lines corresponding to the transitions  ${}^5\text{D}_0 - {}^7\text{F}_j$  ( $j = 1 - 4$ ) of the  $\text{Eu}^{3+}$  ion. Notable peaks occur at 592 nm for the  ${}^5\text{D}_0 - {}^7\text{F}_1$  transition, 613-617 nm for  ${}^5\text{D}_0 - {}^7\text{F}_2$ , 646-652 nm for  ${}^5\text{D}_0 - {}^7\text{F}_3$ , and 694-700 nm for  ${}^5\text{D}_0 - {}^7\text{F}_4$ . Excitation at 470 nm directly stimulates the  $\text{Eu}^{3+}$  ion, inducing the  ${}^7\text{F}_0 - {}^5\text{D}_2$  transition [11-14]. Following this excitation, the electron transitions to the  ${}^5\text{D}_2$  excitation level. Subsequent non-emitting relaxation processes lead the electron to the more stable  ${}^5\text{D}_0$  excited level, and relaxation from this level to the fundamental levels

initiates the fluorescence emission processes as described.

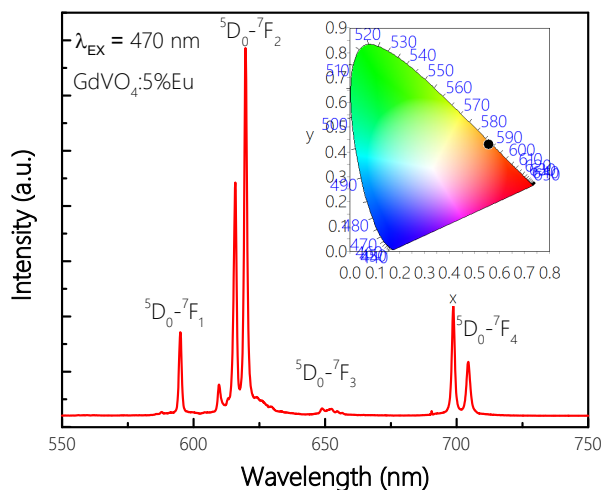


Fig. 4. Emission spectra of  $\text{GdVO}_4:5\%\text{Eu}^{3+}$ . Inset: CIE chromaticity diagram of  $\text{GdVO}_4:5\%\text{Eu}^{3+}$

The CIE (Commission Internationale d'Eclairage) chromaticity coordinates for  $\text{GdVO}_4:5\%\text{Eu}^{3+}$ , derived from the emission spectra, were illustrated in Fig. 4(inset). These coordinates were determined to be  $x=0.5563$  and  $y=0.4306$ , positioning the sample within the pure red region. Additionally, the color temperature and Color Rendering Index (CRI) for this sample were calculated as 1876 K and 81, respectively.

Due to the fact that the chlorophyll spectrum of plants predominantly absorbs light in two regions: blue and red light. Therefore, white light emitting diodes (WLEDs) designed for agricultural purposes must emit light within these specific ranges. To achieve this, WLEDs are produced by blending two powders,  $\text{YAG}:\text{Ce}^{3+}$  and  $\text{GdVO}_4:\text{Eu}^{3+}$ , in a mass ratio of 2:8, and subsequently coating them onto a 470 nm LED chip [1]. The emission spectrum of these WLEDs, as depicted in Fig. 5, demonstrates emission lines within the blue light region (450-475 nm) and red light region (600-700 nm), aligning with the light absorption spectrum of plants. This alignment suggests promising applications for WLEDs in agriculture.

Figure 6 displays the CIE chromaticity diagrams for the WLED device. Its chromaticity coordinates (0.3194, 0.3230) were determined under an excitation wavelength of 470 nm, closely resembling the standard equal energy white light point (0.333, 0.333) [15]. Additionally, this device has a color temperature of 6741 K.

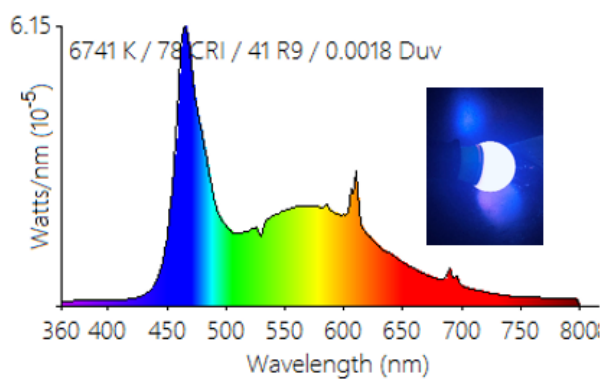


Fig. 5. Emission spectra of WLED device was fabricated by combining  $\text{GdVO}_4:5\%\text{Eu}^{3+}$ ,  $\text{YAG}:\text{Ce}^{3+}$  on LED chip with blue emission 470 nm.

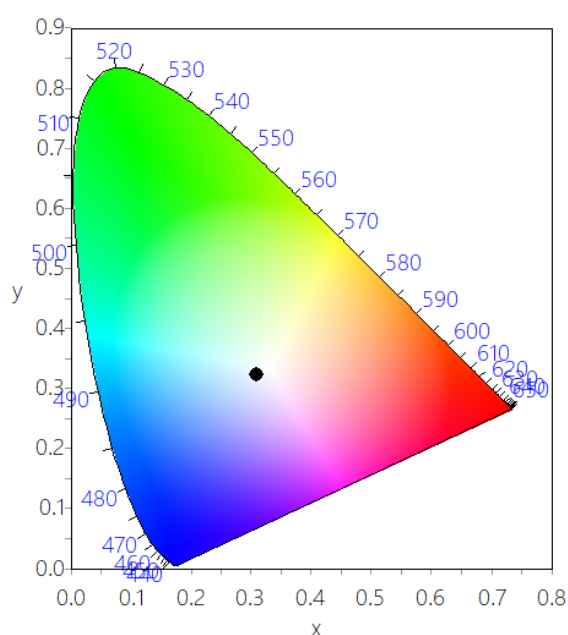


Fig. 6. CIE chromaticity diagram of WLED device

## Conclusion

In summary,  $\text{GdVO}_4:5\%\text{Eu}^{3+}$  was successfully synthesized via the combustion method at  $900^\circ\text{C}$ . The XRD and EDX results indicate the formation of pure  $\text{GdVO}_4$ . According to the PL spectra, under 470 nm excitation,  $\text{GdVO}_4:5\%\text{Eu}^{3+}$  emitted red light in the range of 590 to 700 nm, with chromaticity coordinates of (0.5563, 0.4306). This material, when combined with  $\text{YAG}:\text{Ce}^{3+}$  and LED chip with blue emission 470 nm was tested for creating WLEDs. The emission spectrum of the WLED devices includes both blue and red light regions, making it highly suitable for agricultural applications.

## Acknowledgments

This study is funded in part by the Can Tho University, Code: T2023-73.

## References

1. K. Bi, D. Wang, P. Wang, B. Duan, T. Zhang, Y. Wang, H. Zhang, Y. Zhang, J. Nano. Res. 19 (2017) 174. <https://doi.org/10.1007/s11051-017-3862-2>
2. R. K. Mishra, K. Verma, I. Chianella, H. Y. Nezhad, Next Nanotechnology 5 (2024) 100056. <https://doi.org/10.1016/j.nxnano.2024.100056>
3. M. A. Farooq, F. Hannan, F. Islam, A. Ayyaz, N. Zhang, W. Chen, K. Zhang, Q. Huang, L. Xu, W. Zhou, Environ. Sci. Nano (2022) <https://doi.org/10.1039/D1EN01124C>
4. P. N. Nhi, P. N. Long, T. T. S. Non, V. T. B. Thuy, L. V. Thuc, T. T. Ba, Can Tho University Journal of Science 2 (2016) 1-7. <https://doi.org/10.22144/ctu.jen.2016.008>
5. M. A. Murad, K. Razi, B. R. Jeong, P. M. A. Samy, S. Muneer, Sustainability 13 (2021) 1985. <https://doi.org/10.3390/su13041985>
6. N. Vũ, P. Đ. Roãn, Tạp Chí Hóa Học 53(4E2) (2015) 20-23.
7. K. Lenczewska, Y. Gerasymchuk, N. Vu, N. Q. Liem, G. Boulon, D. Hreniak, J. Mater. Chem. C 3 (2017) 3014. <https://doi.org/10.1039/c6tc04660f>
8. H. Thakur, R. K. Singh, A. K. Gathania, Mater. Res. Express 8 (2021) 026201. <https://doi.org/10.1088/2053-1591/abe221>
9. S. Han, Y. Du, J. Yuan, Y. Tao, Y. Wang, S. Yan, Danping Chen, Journal of Non-Crystalline Solids 532 (2020) 119894. <https://doi.org/10.1016/j.jnoncrsol.2020.119894>
10. D. J. Jovanovic, Z. Antic, R. M. Krsmanovic, M. Mitric, M. D. Dramicanin, Optical Materials, 35 (2013) 1797-1804. <http://dx.doi.org/10.1016/j.optmat.2013.03.012>
11. K. K. M. Ngo, V. Nguyen, T. K. G. Lam, T. K. Hoang, M. T. Dinh, M. Stefanski, K. Grzeszkiewicz, D. Hreniak, Int. J. Nanotechnol., 17 (2020) 623-635. <https://doi.org/10.1504/IJNT.2020.111329>
12. N. K. K. Minh1, T. B. Luan, L. T. K. Giang, N. T. Thanh, T. T. K. Chi, D. Hreniak, N. Q. Luan, N. Vu, Materials Transactions 61(8) (2020) 1564-1568. <https://doi.org/10.2320/matertrans.MT-MN2019027>
13. N. K. K. Minh, N. Q. Luân, P. T. Phưởng, P. T. Tùng, L. T. K. Giang, N. Vũ, Vietnam Journal of Catalysis and Adsorption, 12 (2023) 106-110. <https://doi.org/10.51316/jca.2023.017>
14. M. Toro-González, R. Copping, S. Mirzadeh, J. V. Rojas, J. Mater. Chem. B, 6 (2018) 7985. <https://doi.org/10.1039/c8tb02173b>
15. X. Li, Y. Wei, P. Dang, X. Xiao, H. Xiao, G. Zhang, G. Li, J. Lin, Materials Research Bulletin 146 (2022) 111592. <https://doi.org/10.1016/j.materresbull.2021.111592>